Thermal Fluid Transport Phenomena in Concentric Annulus with Movement and Rotation of Inner Core

S. Torii[1]

Abstract: A numerical study is performed to investigate the thermal fluid-flow transport phenomena in the concentric annulus with a slightly heated rotating inner core moving in the flow direction and a stationary insulated outer cylinder. Emphasis is placed on the effects of the axial rotation and streamwise movement of inner core on the flow structure and heat transfer performance. A k-ε turbulence model is employed to determine the turbulent viscosity and the turbulent kinetic energy. The turbulent heat flux is expressed by Boussinesq approximation in which the eddy diffusivity for heat is determined using two-equation heat transfer model. The governing equations are discretized by means of a control volume finite-difference technique and numerically solved. An inner core rotation causes amplification of the turbulent kinetic energy over the whole cross section, resulting in a substantial enhancement in the Nusselt number. This trend is suppressed due to the inner core movement. The streamwise movement of the inner core causes substantial reductions in the turbulent kinetic energy intensified by the inner core rotation, resulting in the deterioration of heat transfer performance. Heat transfer characteristics in Couette flow in concentric annulus are found to be affected by both the velocity ratio of the moving inner cylinder to the fluid flow and the inner core rotating speed.

keyword: turbulent Couette flow, moving core in concentric annuli, inner core rotation, Nusselt number, turbulent kinetic energy

1 Introduction

Annular flow geometry is encountered in many important engineering applications. The problems of heat transfer and fluid flow can be classified into three categories:

(i) stationary cylinder case, (ii) circular Couette flow case, and (iii) parallel Couette flow case. In particular, the circular Couette flow, i.e., swirling flow, implies a flow with one surface rotating and the other stationary (or both surfaces rotating in the same direction at different angular velocities). Problems involving transport phenomena in swirling flows can be found in chemical and mechanical mixing or separation devices, electric and turbo-machinery, combustion chambers, pollution control devices, swirl nozzles, and fusion reactors. Furthermore, the parallel Couette flow refers to a flow in an annulus with one surface moving in the flow direction and the other remaining stationary (or both surfaces moving in the flow direction at different velocities). This type flow is seen in railway tunnels such as the 54 km long Seikan tunnel in Japan and the England Channel tunnel. As for these two Couette flows, numerous experimental and theoretical studies have been performed on the thermal fluid flow transport phenomena in a concentric annulus [for example, Kuzay and Scott (1975 and 1976); Hirai et al. (1987); Lee and Kim (1987); and Shigechi et al. (1990); Torii and Yang (1994a and b)].

Recently, Marques and Lopez (1997) studied the stability of isothermal parallel Couette flow with axial oscillations of the inner cylinder using Floquet theory. Furthermore, the stability of Couette flow in concentric annulus, in which the outer cylinder is stationary and the axially rotating inner core moves with a constant speed along the axial direction, was investigated by Ali (2000). He disclosed that the constant axial movement of the inner cylinder stabilizes the flow and the critical parameters at the onset of instability are determined based on the axial velocity of the inner cylinder. To the author's knowledge, there are no experimental and numerical results on the thermal fluid-flow transport phenomenon in this annular configuration, although some modern numerical methods have been developed which are applicable for this problem [Wu, Senocak, Wang, Wu, and Shyy(2003), Tsai, Young and Cheng(2002)].

This paper treats the thermal transport phenomenon in

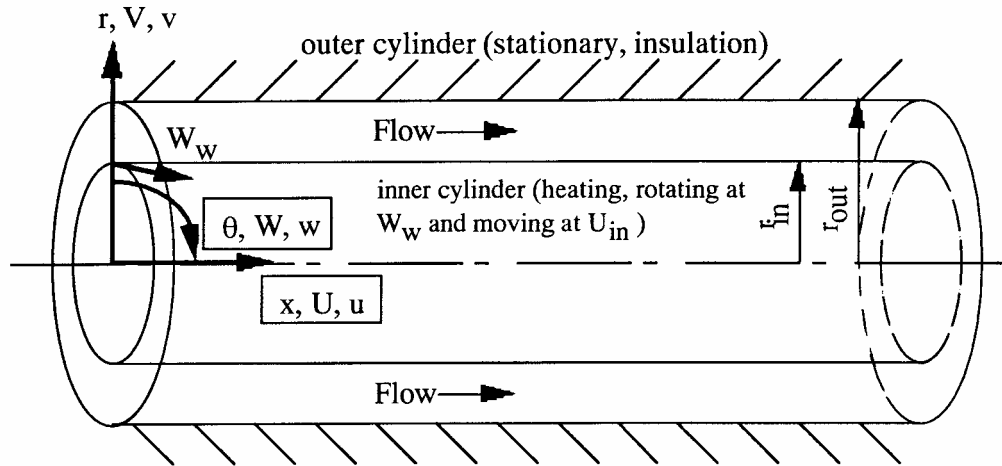[1] Department of Mechanical Engineering, Kagoshima University, Kagoshima, 890-0065, JAPAN

Figure 1 : A schematic of physical system and coordinate.

the Couette flow between a concentric annulus with the outer one stationary and the inner one rotating and also moving along the axis with a constant velocity. Consideration is given to the effects of the streamwise movement and axial rotation of the inner core on heat transfer rate and the velocity and thermal fields, i.e., streamwise and tangential velocity profiles, turbulent kinetic energy, temperature variance, and turbulent heat flux. Numerical results are obtained using the k-ε turbulence model and two-equation heat transfer model.

2   Governing Equations and Numerical Scheme

Consider a forced flow through a concentric annulus consisting of a stationary insulated outer cylinder and an axially rotating and steamwise moving inner cylinder under a uniform flux heating condition. The physical configuration and the cylindrical coordinate system are schematically shown in Fig. 1. The following assumptions are imposed in the formation of the problem: incompressible, turbulent, steady-state flow; constant fluid properties; and negligible axial conduction (due to the high Peclet number). There are no variations in tangential direction, because cylindrical symmetry. Since the buoyancy parameter Gr/Re^2 is less than 0.1, forced convection dominates. Hence, the continuity, momentum, and energy equations, with neglect of the buoyancy force, read in the tensor formation as:

Continuity equation:

$$\frac{\partial U_i}{\partial x_i} = 0 \tag{1}$$

Momentum equation:

$$U_j \frac{\partial U_i}{\partial x_j} = -\frac{1}{\rho}\frac{\partial P}{\partial x_i} + \frac{\partial}{\partial x_j}\left[\nu\left(\frac{\partial U_i}{\partial x_j} + \frac{\partial U_j}{\partial x_i}\right) - \overline{u_i u_j}\right] \tag{2}$$

Energy equation:

$$U_i \frac{\partial T}{\partial x_i} = \frac{\partial}{\partial x_i}\left(\alpha \frac{\partial T}{\partial x_i} - \overline{u_i t}\right) \quad . \tag{3}$$

Here U_i and T are time-averaged velocity component in the x_i direction and time-averaged temperature, respectively. α is thermal diffusivity. By using Boussinesq's approximation, the Reynolds stress $-\overline{u_i u_j}$ in Eq. (2) is expressed as:

$$-\overline{u_i u_j} = -\frac{2}{3}k\delta_{ij} + \nu_t\left(\frac{\partial U_i}{\partial x_j} + \frac{\partial U_j}{\partial x_i}\right) \quad . \tag{4}$$

Here, the turbulent viscosity ν_t in Eq. (4) is related to the turbulent kinetic energy k and its dissipation rate ε through Kolmogorov-Prandtl's relation [Rodi (1982)], as

$$\nu_t = C_\mu f_\mu \frac{k^2}{\varepsilon} \quad , \tag{5}$$

where C_μ is a model constant and f_μ is a model function. The turbulent heat flux $-\overline{u_i t}$ in Eq. (3) can be expressed in the following form:

$$-\overline{u_i t} = \alpha_t \frac{\partial T}{\partial x_i}$$
$$= C_\lambda f_\lambda k \sqrt{\frac{k\,\overline{t^2}}{\varepsilon\,\varepsilon_t}} \frac{\partial T}{\partial x_i} \quad , \tag{6}$$

where C_λ is a model constant and f_λ is a model function. α_t is turbulent thermal diffusivity. In order to evaluate k, ε, $\overline{t^2}$ and ε_t in Eq. (6), a low-Reynolds number version of k-ε turbulence model and the two-equation heat-transfer model are used in the present study. The transport equations of k and ε are expressed in Cartesian tensor form [Torii et al. (1991)]:

$$U_j \frac{\partial k}{\partial x_j} = \frac{\partial}{\partial x_j}\left[\left(\nu + \frac{\nu_t}{\sigma_k}\right)\frac{\partial k}{\partial x_j}\right]$$
$$-\overline{u_i u_j}\frac{\partial U_i}{\partial x_j} - \varepsilon - 2\nu\left(\frac{\partial \sqrt{k}}{\partial x_j}\right)^2 \tag{7}$$

$$U_j \frac{\partial \varepsilon}{\partial x_j} = \frac{\partial}{\partial x_j}\left[\left(\nu + \frac{\nu_t}{\sigma_\varepsilon}\right)\frac{\partial \varepsilon}{\partial x_j}\right]$$
$$- C_1 f_1 \frac{\varepsilon}{k}\overline{u_i u_j}\frac{\partial U_i}{\partial x_j} - C_2 f_2 \frac{\varepsilon^2}{k}$$
$$+ \nu \nu_t \left(1 - f_\mu\right)\left(\frac{\partial^2 U_i}{\partial x_j^2}\right)^2 \tag{8}$$

The empirical constants and model functions in Eqs. (5), (7) and (8) are listed in Table 1. The transport equations for temperature variance $\overline{t^2}$ and its dissipation rate ε_t are expressed as:

$$U_j \frac{\partial \overline{t^2}}{\partial x_j} = \frac{\partial}{\partial x_j}\left[\left(\alpha + \frac{\alpha_t}{\sigma_h}\right)\frac{\partial \overline{t^2}}{\partial x_j}\right] - 2\overline{u_j t}\frac{\partial T}{\partial x_j}$$
$$- 2\varepsilon_t - 2\alpha\left(\frac{\partial \sqrt{\overline{t^2}}}{\partial x_j}\right)^2 \tag{9}$$

and

$$U_j \frac{\partial \varepsilon_t}{\partial x_j} = \frac{\partial}{\partial x_j}\left[\left(\alpha + \frac{\alpha_t}{\sigma_\phi}\right)\frac{\partial \varepsilon_t}{\partial x_j}\right] +$$
$$C_{p1} f_{p1} \frac{\varepsilon\alpha_t}{k}\left(\frac{\partial T}{\partial x_j}\right)^2 + C_{p2} f_{p2}\frac{\varepsilon_t \nu_t}{k}\left(\frac{\partial U}{\partial x_j}\right)^2$$
$$- C_{D1} f_{D1}\frac{\varepsilon_t^2}{\overline{t^2}} - C_{D2} f_{D2}\frac{\varepsilon\varepsilon_t}{k} + \alpha\alpha_t\left(1 - f_t\right)\left(\frac{\partial^2 T}{\partial x_j}\right)^2 \tag{10}$$

respectively. The empirical constants and model functions in Eqs. (6), (9) and (10) are listed in Table 2. Notice that the original model function in each turbulence model is slightly modified so as to simulate the transition from turbulent to laminar flows, whose modification process is described in reference [Torii et al. (1991); Torii and Yang (1997)]. Although Youssef et al. (1992) point out that the original two-equation heat transfer model does not precisely reproduce the wall limiting behavior of turbulence quantities in a thermal field under arbitrary wall thermal conditions, the present study employs this heat transfer model, because the model gives the proper information on the thermal transport phenomenon.

A set of the governing equations is solved using the control-volume based formulation of Patankar (1980). In this procedure, the domain is discretized by a series of control volumes, with each control volume containing a grid point. Each differential equation is expressed in an integral manner over the control volume, and profile approximations are made in each coordinate direction, leading to a system of algebraic equations that can be solved in an iterative manner. A power law interpolation scheme is used to evaluate the values of variables at the control volume interfaces. The discretized equations are solved with a line-by-line and the TDMA (tridiagonal-matrix algorithm). The convergence criteria of the residuals of all equations are assumed to be less than 10^{-5} of total inflow rates. Since all turbulent quantities, as well as the time-averaged streamwise velocity, vary rapidly in the near-wall region, the size of nonuniform cross-stream grids is increased with a geometric ratio from the wall toward the center region of the annulus. This is because the nonuniform cross-stream grids save CPU time and the accuracy is maintained in the vicinity of the wall. The maximum control volume size near the center regime is always kept at less than 3% of the hydrodynamic tube radius. In order to ensure the accuracy and validity of calculated results, at least two control volumes are positioned in the viscous

C_μ	C_1	C_2	σ_κ	σ_ε	f_1	f_2	f_μ
0.09	1.44	1.9	1.0	1.3	$1+0.28\exp\left(-\frac{R_t}{25}\right)$	$1-0.3\exp\left(-R_t^2\right)$	$\left\{1-\exp\left(\frac{-R_\tau}{26.5}\right)\right\}^2$

Table 1 : Empirical constants and model functions in the k-ε model.

C_λ	C_{P1}	C_{P2}	σ_h	σ_ϕ	C_{D1}	C_{D2}	f_{P1}	f_{P2}	f_{D1}	f_{D1}	f_λ
0.11	1.80	0.72	1.0	1.0	2.20	0.80	1.0	1.0	1.0	1.0	$\left\{1-\exp\left(-\frac{\sqrt{P_r}}{30.5}\frac{2}{f}St\,y^+\right)\right\}^2$

Table 2 : Empirical constants and model functions in the $\overline{t^2}$-ε_t heat-transfer model.

sublayer, i.e., $y^+ <5$. Since the velocity and temperature fields are decoupled for non-bouyant flows, the velocity field can be solved first, followed by the temperature field. The discretized equations are solved from the inlet in the downstream direction by means of a marching procedure, since the equations employed here are parabolic. A length of 180 diameters is employed and their volumes in the streamwise direction are distributed uniformly.

A hydrodynamically fully-developed isothermal annular flow in the absence of the inner core rotation is assumed at the inlet location, i.e., at the onset of heating. The following boundary conditions are used at the wall:

$r = r_{in}$: $U = U_{in}$, $k = 0$, $W = W_w$, $\varepsilon=0$,
$\varepsilon_t = 0$, $\overline{t^2} = 0$, $\frac{\partial T}{\partial r} = -\frac{q_w}{\lambda_w}$
$r = r_{out}$: $U = k = 0$, $W = 0$, $\varepsilon = 0$,
$\varepsilon_t = 0$, $\overline{t^2} = 0$, $\frac{\partial T}{\partial r} = 0$

Here, r_{in} and r_{out} are inner and outer radii of the annulus, respectively. And U_{in} is velocity of a moving inner cylinder and W_w is tangential velocity on the inner cylinder. For annular flows with a rotating inner surface and/or a streamwise moving inner surface, the axial and tangential flow fields are also governed by dimensionless parameters including radius ratio, r* ($=r_{in}/r_{out}$), the velocity ratio of inner core and fluid flow, N, inlet Reynolds number (i.e., Reynolds number at the onset of heating), Re, and Taylor number, Ta. N, Re and Ta are defined as

$$N = \frac{U_{in}}{u_m}, \quad Re = \frac{2\,u_m\,(r_{out}-r_{in})}{\nu} \quad,$$
$$\text{and} \quad Ta = \frac{W_w\,(r_{out}-r_{in})}{\nu}\sqrt{\frac{r_{out}-r_{in}}{r_{in}}}, \quad (11)$$

respectively. Here u_m denotes mean velocity over channel cross section. The dimensionless parameters are r*=0.8; N¡1.0; Re=3000-10000; Ta=0~10000; inlet gas

(nitrogen) temperature T_{inlet}=273 K.

Simulations with grids of various degrees of coarseness are conducted to determine the required resolution for grid-independent solutions. Throughout the numerical calculations, the number of control volumes is properly selected between 60 and 120 over the cross-section of the concentric annulus. Consequently, the maximum error was estimated to be about 0.5% by comparing the solutions on regular and fine grids with twice the grid points in the radial direction. Numerical computation was performed on a personal computer (Pentium IV CPU 1.7GHz).

In order to verify the k-ε turbulence and the two-equation heat-transfer models and to determine the reliability of the computer code developed here, numerical predictions are compared with some existing experimental results in both the thermal and flow fields. The models are applied to a flow in an annulus (r*=0.56) with a stationary inner cylinder with a uniform wall heat flux. Numerical results are obtained at a location of 220 times the tube diameter downstream from the inlet where both thermally- and hydrodynamically-fully developed conditions prevail.

Figure 2 depicts the predicted time-averaged streamwise velocity profile together with the experimental data at Re=46000 obtained by Brighton and Jones(1964). Here, Figs. 2(a) and (b) correspond to the distributions from the inner and outer walls to the location of the maximum streamwise velocity, respectively. The calculation result agrees with the experimental results, representing the well-known characteristics in the logarithmic region. In Fig. 3, the calculated turbulent kinetic energy is compared with the experimental data [Brighton and Jones (1964)] at Re=46000. The predicted results are normalized by the square of the friction velocity on the outer wall, $(u*_{out})^2$. The turbulence model predicts well in the outer region, but its accuracy deteriorates near the inner

wall. That is, the turbulent kinetic energy is slightly over-estimated in the vicinity of the inner core.
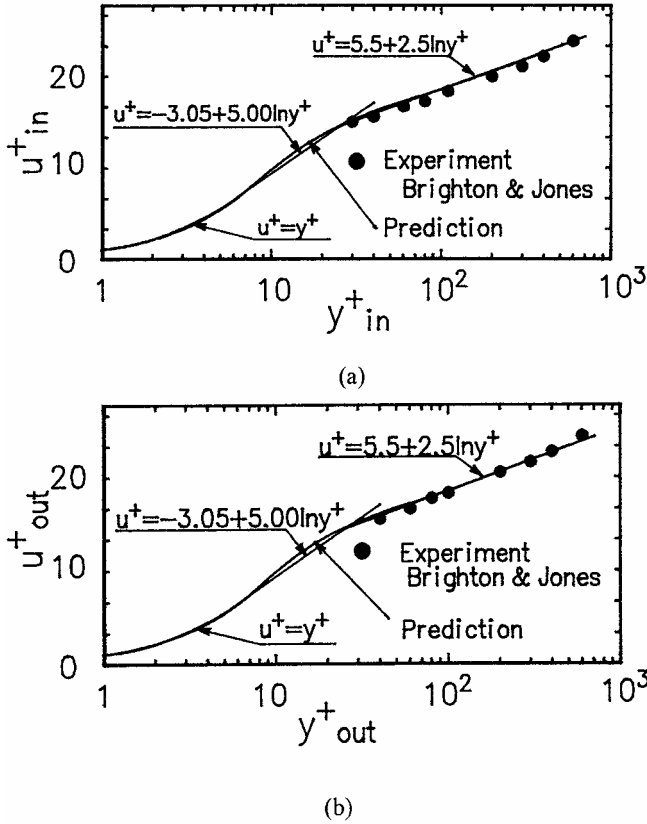

(a)

(b)

Figure 2 : Distribution of predicted time-averaged streamwise velocity in stationary concentric annulus for Re=46000 and r*=0.56, (a) inner side and (b) outer side.
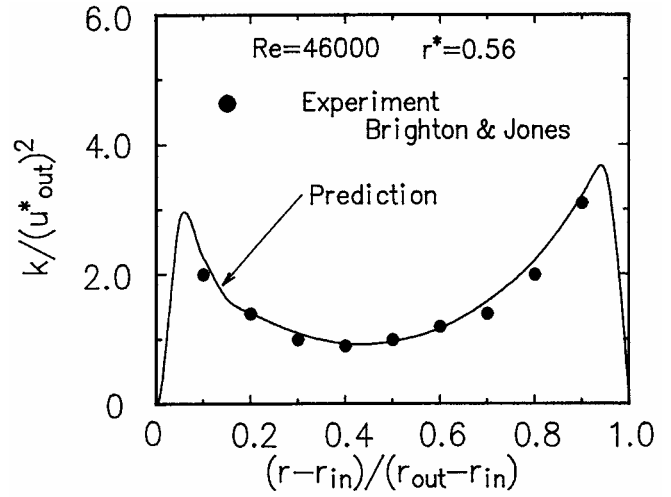

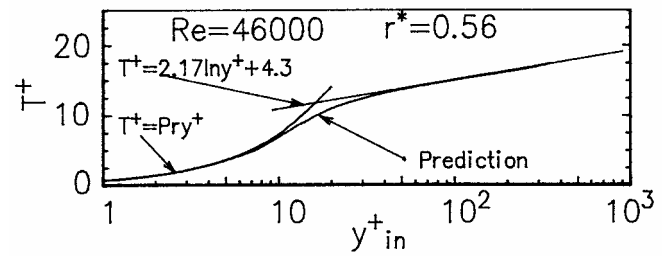**Figure 3** : Distribution of predicted turbulent kinetic energy in stationary concentric annulus for Re=46000 and r*=0.56.

Figure 4 : Dimensionless time-averaged temperature distribution in stationary concentric annulus for Re=46000 and r*=0.56.

The predicted radial distribution of the time-averaged temperature in the inner wall region at Re=46000 is illustrated in Fig. 4 in the form of T^+ versus y_{in}^+. T^+ is dimensionless time-averaged temperature and y_{in}^+ denotes the dimensionless distance measured from the heated inner core wall. It is observed that the two-equation heat transfer model reproduces the law of the wall for a thermal boundary layer. The validity of the computer code and the validity of both the k-ε turbulence and two-equation heat transfer models are borne out through the above comparisons.

3 Results and Discussion

Figure 5, for N=0, illustrates numerical results of the Nusselt number Nu at different Taylor numbers. Dalle

Donne and Meerwald (1966) derives the following correlation for the Nusselt number at the inner wall of the annulus as:

$$Nu = 0.0181 \left(\frac{r_{out}}{r_{in}}\right)^{0.2} Re^{0.8} \Pr^{0.4} \left(\frac{T_{win}}{T_{inlet}}\right)^{-0.18} \quad (12)$$

This equation is superimposed in Fig. 5 as a solid straight line. Notice that Fig. 5 is under the temperature ratio of the inner wall to the inlet fluid, T_{win}/T_{inlet}, of unity, and the radius ratio, r*, of 0.8. It is seen that the prediction at Ta=0 is in good agreement with the correlation. One observes that the Nusselt number increases with an increase in the Taylor number. This trend becomes larger in the low Reynolds number region. It is found that an amplification of heat transfer performance in concentric annulus

in the absence of inner core movement is attributed to the axial rotation of the inner cylinder and the enhanced level is affected by the Reynolds number.
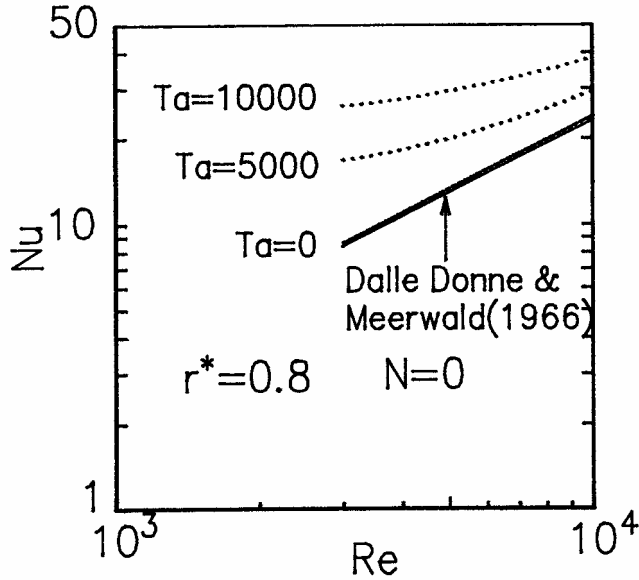

Figure 5 : Variation of predicted Nusselt numbers in circular Couette flow for r*=0.8 and N=0.

Meanwhile, the effect of inner core movement on the enhanced heat transfer rate as seen in Fig. 5 is depicted in Fig. 6 in the form of the Nusselt number versus the Reynolds number with the velocity ratio N, as a parameter. Numerical results are obtained at Ta=5000. The prediction at Ta=5000 in Fig. 5 is superimposed in the figure. It is observed that enhancement of heat transfer performance due to the axial inner core rotation is suppressed by the streamwise movement of the inner core. This deterioration is intensified with an increase in the velocity ratio and the same trend yields in the wide range of the Reynolds number. In other words, the Nusselt number, which is intensified by the inner core rotation, is substantially diminished by the inner core movement in the flow direction. It is found that heat transfer performance in Couetter flows is affected by both of streamwise movement and axial rotation of inner and its rate is determined by the combination of the Reynolds number, the Taylor number and the velocity ratio.

Figure 7 illustrates the effects of Taylor number and velocity ratio on the heat transfer rate. The numerical results for Re=8000 are depicted in the form of Ta versus Nu/Nu_f with the velocity ratio, as a parameter. Here,
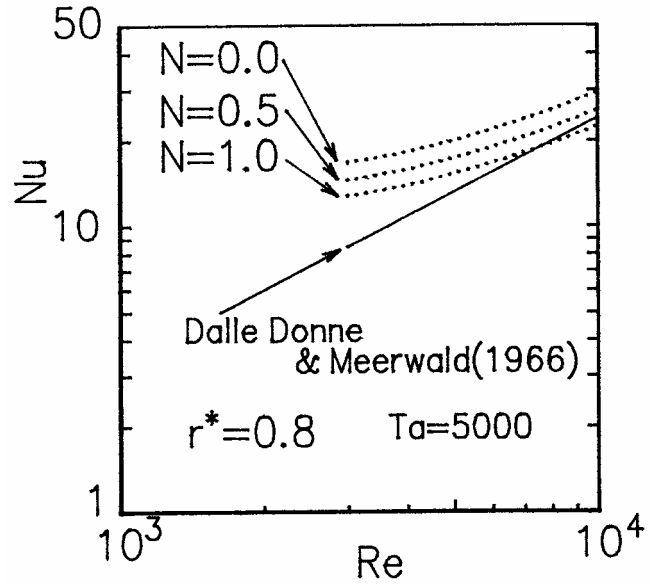
Nu_f denotes the Nusselt number for a fully-developed turbulent annular flow in the absence of the axial rotation and streamwise movement of the inner core. It is observed that at N fixed, the Nusselt number increases with an increase in the Taylor number. The heat transfer enhancement is suppressed by the inner core movement and the uniform deterioration yields over the whole region of the Taylor number as the velocity ratio is increased.
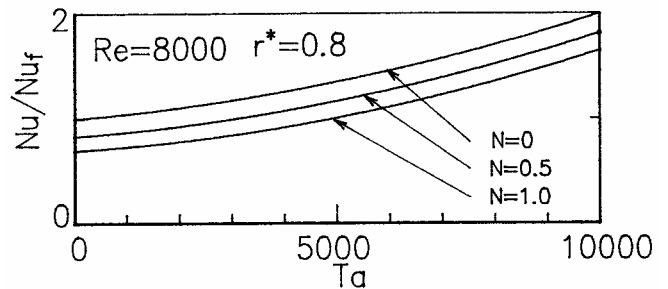

Figure 6 : Effect of velocity ratio on Nusselt numbers in circular Couette flow, for r*=0.8 and Ta=5000.

Figure 7 : Effects of Taylor number and velocity ratio on Nusselt number in Couette flow at r*=0.8 and Re=8000.

An attempt is made to explore the mechanisms of transport phenomena of circular Couette flows with a streamwise inner core movement in a concentric annulus based on numerical results at Re=8000. Figures 8(a) and (b) show the radial distributions of streamwise and tangential

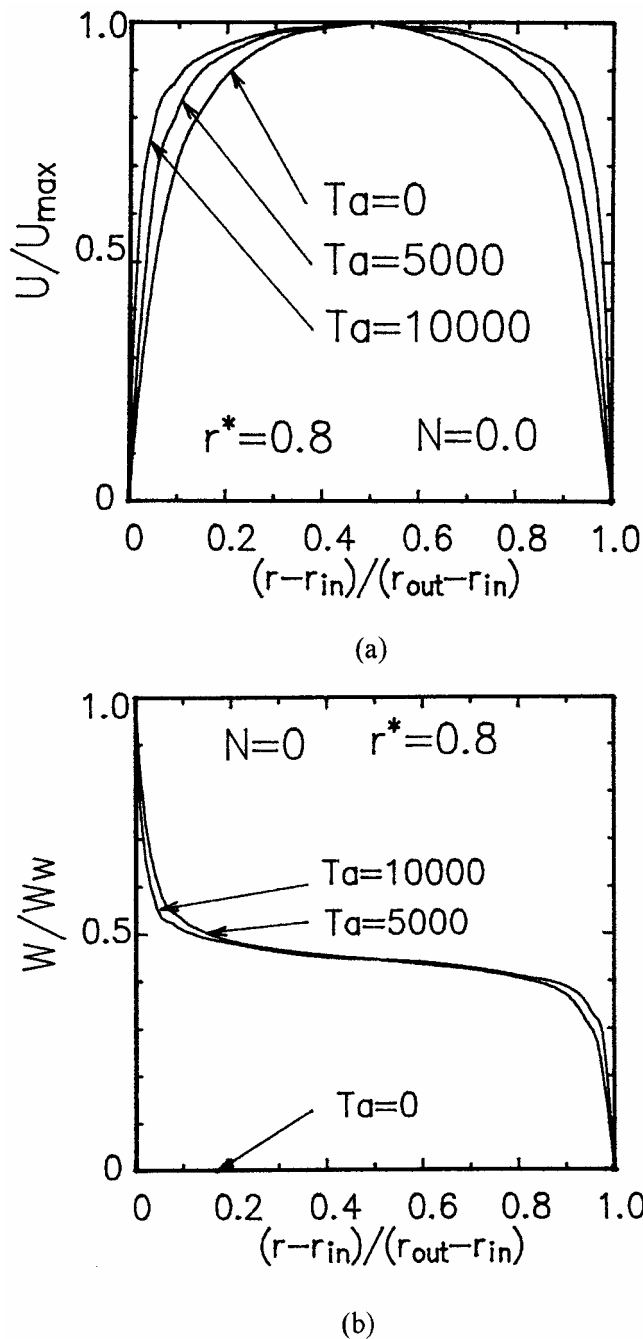(a)

(b)

Figure 8 : Variation of time-averaged velocity profiles in circular Couette flow for r*=0.8, N=0 and Re=8000, (a) streamwise velocity and (b) tangential velocity.

velocities in the annulus in the absence of the inner core movement, respectively. In both figures, the velocities at Ta=0, 5000 and 10000 are normalized by its maximum value at each Taylor number. The streamwise velocity

profile at Ta=0 shows a turbulent annular flow in the absence of rotation, as seen in Fig. 8(a). The corresponding tangential velocity in Fig. 8(b) is zero over the flow cross section. One observes that the streamwise velocity gradient increase near the inner and outer walls due to the inner core rotation and its presence causes the swirling flow. The corresponding radial variation of the turbulent kinetic energy is illustrated in Fig. 9 with a change in Ta. The numerical results are divided by the square of the friction velocity, u*, on the outer wall for the annular flow without the swirl. The turbulent kinetic energy near the wall region is induced with an increase in Ta. In particular, this trend becomes larger in the vicinity of the inner wall. These behaviors are in accord with the variations of the streamwise and tangential velocities in Figs. 8(a) and (b). In other words, an increase in the streamwise velocity gradient in the vicinity of walls and the presence of the tangential velocity cause an amplification of the production of the turbulent kinetic energy.
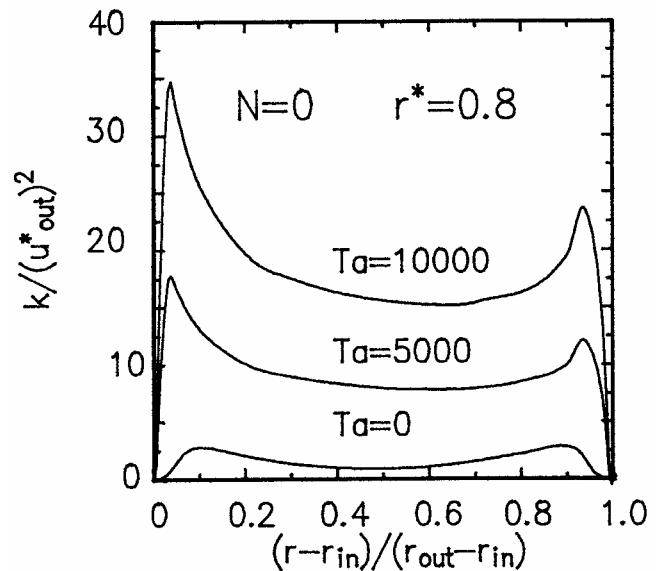

Figure 9 : Predicted turbulent kinetic energy profiles in circular Couette flow for r*=0.8, N=0 and Re=8000.

The effect of inner core movement on the changes in the streamwise and tangential velocities is illustrated in Figs. 10(a) and (b), respectively. Here, both velocities at Ta=5000 in Figs. 8(a) and (b) are superimposed in the figures for comparison. It is observed that as N is increased, the peak of U/U_{max} shifts toward the inner cylinder side, resulting in a substantial deformation of the ve-

locity profile of the fully developed circular Couette flow, as seen in Fig. 10(a). This implies that the intensified velocity gradient at the inner wall is significantly diminished by the streamwise movement of the inner cylinder, with only a slight change in the outer wall region. Similarly, the velocity gradient of the tangential velocity at the inner wall is also attenuated due to the inner core movement, as shown in Fig. 10(b). The corresponding effect of inner core movement on the turbulent kinetic energy in the circular Couetter flow is illustrated in Fig. 11 in the same form as Fig. 9 with N, as a parameter. Numerical results are obtained at Ta=5000. One observes that (i) the inner core movement suppresses the turbulent kinetic energy level over the annular cross-section, and (ii) this effect becomes larger in the vicinity of the streamwise moving inner core wall. Thus this variation ascribes to attenuation in the streamwise and tangential velocity gradients, as seen in Figs. 10(a) and (b). In other words, substantial attenuation in the velocity gradients suppresses the production of turbulence, resulting in deterioration of the turbulent kinetic energy.

The radial distribution of the temperature variance, $\overline{t^2}$, in the thermal field in the annulus with the stationary core is illustrated in Fig. 12 as a function Ta. Here, the numerical results are normalized by the square of the friction temperature, t^*, for the annular flow without the inner core rotation. As the Taylor number increases, the temperature variance enhances in the whole flow cross section, particularly in the vicinity of the rotation wall. The radial distribution of the turbulent heat flux is depicted in Fig. 13 as a function of Ta. Here, the numerical results are normalized by the product of the friction temperature t^* and the friction velocity u^*_{out} on the outer wall for the annular flow in the absence of inner core rotation. The turbulent heat flux level in the vicinity of the inner wall is substantially augmented with an increase in Ta.

The corresponding radial distributions of the temperature variance $\overline{t^2}$ in the circular Couettte flow with inner core movement are illustrated in Fig. 14 in the same form as Fig. 12. Here, numerical result at Ta=5000 in Fig. 12 are superimposed in the figures for comparison. As the flow moves, there is a reduction in $\overline{t^2}$ for N=1 over the whole cross section and this trend becomes larger in the vicinity of the heated moving wall, as seen in Fig. 14. This behavior implies attenuation in the temperature fluctuations in the thermal field. Figure 15, for Ta=5000, shows the radial distribution of the turbulent heat flux as
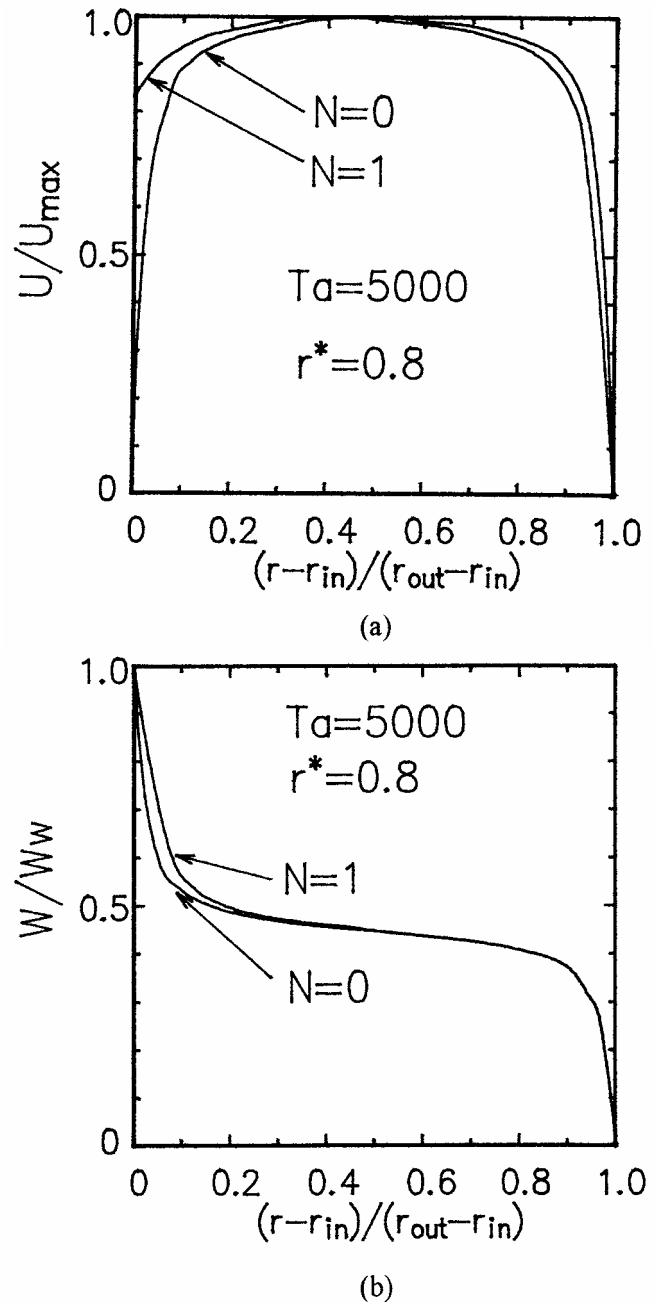

(a)

(b)

Figure 10 : Effect of velocity ratio on velocity profiles in circular Couette flow, for r*=0.8, Ta=5000 and Re=8000, (a) streamwise velocity and (b) tangential velocity.
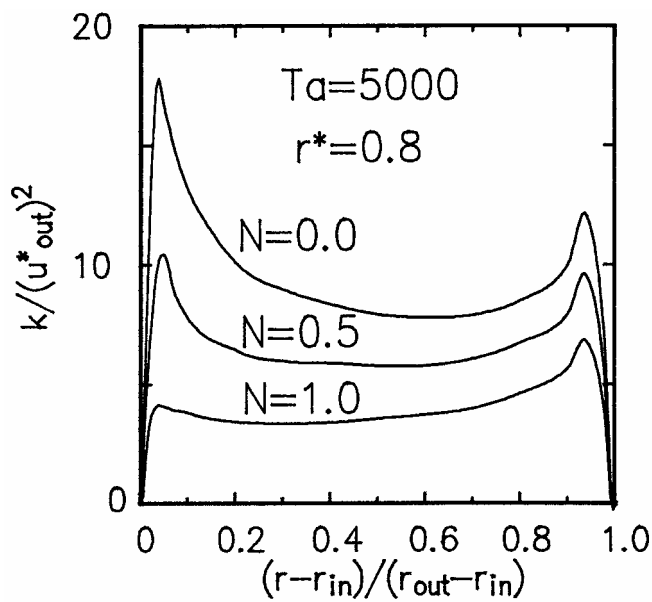
a function of N.

Figure 11 : Effect of velocity ratio on turbulent kinetic energy profiles in circular Couette flow for r*=0.8, Ta=5000 and Re=8000.

Figure 12 : Effect of Taylor number on radial distribution of temperature variance in circular Couette flow at Re=8000, N=0 and r*=0.8.

One observes that (i) the turbulent heat flux intensified by the inner core rotation is attenuated by the streamwise movement of the inner core, and (ii) in particular, its level in the vicinity of the inner wall is substantially decreased with an increase in N.

Since the eddy diffusivity concept is employed to determine the turbulent heat flux $-c_p \overline{\rho} \, \overline{vt}$ in Eq. (3), λ_t is directly related to k, ε, $\overline{t^2}$ and ε_t as depicted in Eq. (6). Hence, substantial amplifications in the turbulent kinetic energy and temperature variance result in enhancement in the Nusselt number, as shown in Fig. 5. In contrast, the deterioration of k and $\overline{t^2}$, suppresses heat transfer performance, as seen in Fig. 6.

4 Conclusions

The k-ε turbulence model and two-equation heat transfer model have been employed to numerically investigate the fluid flow and heat transfer in concentric annuli with a slightly heated rotating inner core moving in the flow direction and a stationary insulated outer cylinder. Consideration is given to the effect of inner core movement on the flow and thermal fields in circular Couette flows. Results are summarized as follows:
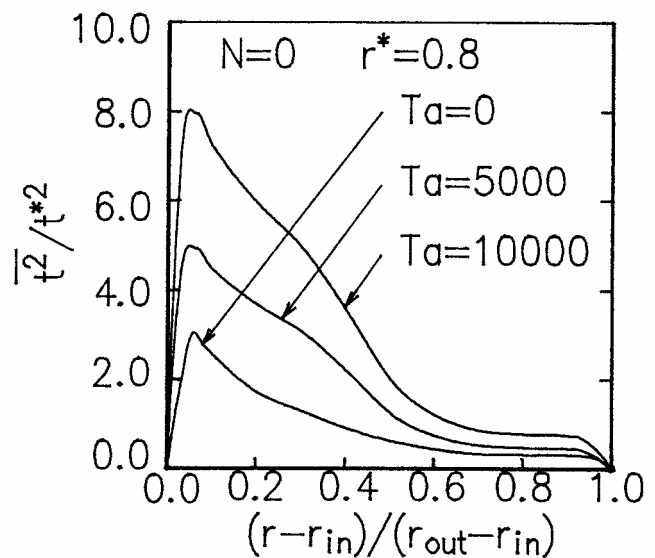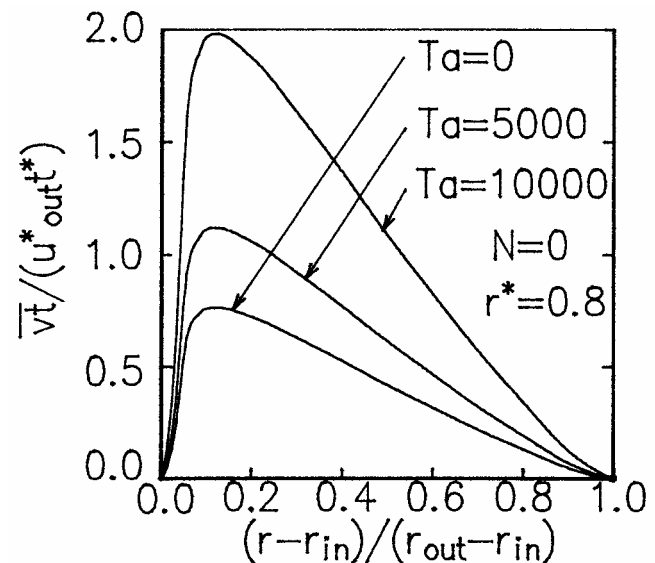

Figure 13 : Effect of Taylor number on radial distribution of turbulent heat flux in circular Couette flow at Re=8000, N=0 and r*=0.8.

1 The turbulence models of heat and momentum predict an increase in the Nusselt number due to an axially rotating inner cylinder. The streamwise and tangential velocity gradients in the vicinity of the inner and outer cylinder walls are increased due to the inner core rotation. The amplification of the turbulent kinetic energy and temperature variance intensifies the turbulent heat flux, resulting in an enhancement in heat transfer performance.

2 The intensified heat transfer rate in the annulus in the presence of the inner core rotation is substantially attenuated by the streamwise movement of the inner cylinder. The inner core movement causes a suppression of the velocity gradients of the streamwise and tangential velocities near the inner wall and attenuation in both the turbulent kinetic energy and the temperature variance. Consequently, these variations induce a decrease in the turbulent heat flux, resulting in the deterioration of heat transfer performance.
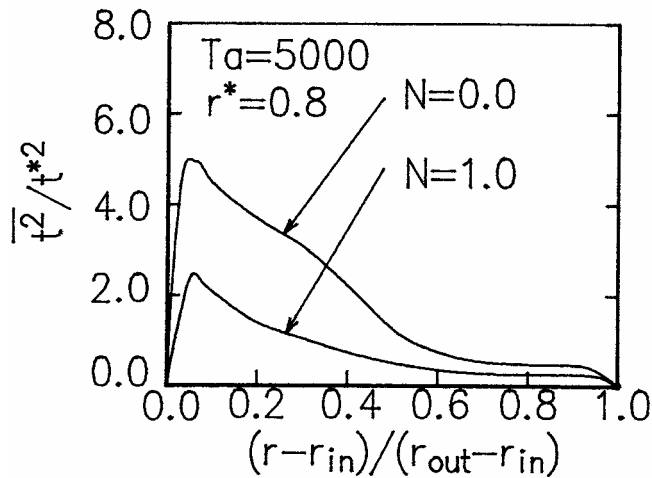

Figure 14 : Effect of velocity ratio on radial distribution of temperature variance in circular Couette flow at Re=8000, Ta=5000 and r*=0.8.
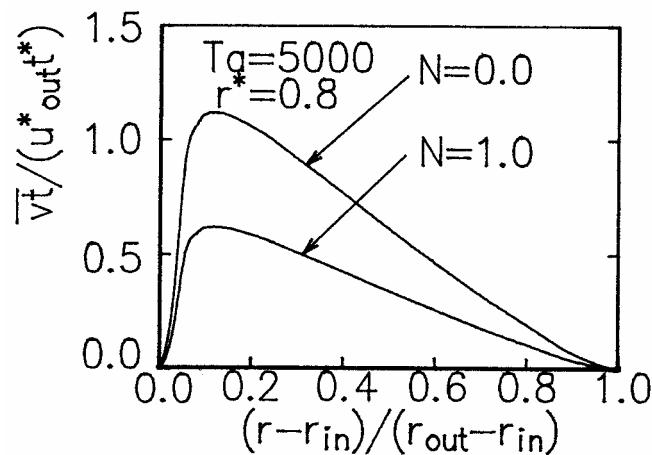

Figure 15 : Effect of velocity ratio on radial distribution of turbulent heat flux in circular Couette flow at Re=8000, Ta=5000 and r*=0.8.

References

Ali, M. A. (2000): The stability of Couette flow with an inner cylinder rotating and moving with a constant axial velocity, *Fluid Dynamics Research*, vol. 27, pp. 109-115.

Brighton, J. A.; Jones, J. B. (1964): Fully developed turbulent flow in annuli, *Trans. of ASME*, D, pp. 835-844.

Dalle Donne, M.; Meerwald, E. (1966): Experimental Local Heat Transfer and Average Friction Coefficients for Subsonic Turbulent Flow of Air in an Annulus at High Temperatures, *Int. J. Heat Mass Transfer*, vol. 9, pp. 1361-1376.

Hirai, S.; Takagi, T.; Tanaka, K.; Kida, K. (1987): Effect of Swirl on the Turbulent Transport of Momentum in a Concentric Annulus with a Rotating Inner Cylinder, *Trans., JSME*, vol. 53, no. 486, pp. 432-437 (in Japanese).

Kuzay, T. M.; Scott, C. J. (1975): Turbulent Heat Transfer Studies in Annulus with Inner Cylinder Rotation, *Trans. of ASME*, 75-WA/HT-55, pp. 1-11.

Kuzay, T. M.; Scott, C. J. (1976): Turbulent Prandtl Numbers for Fully Developed Rotating Annular Axial Flow of Air, *Trans. of ASME*, 76-HT-36, pp. 1-13.

Lee, Y.; Kim, K. H. (1987): Inverted annular film boiling, *Int. J. Multiphase Flow*, vol. 13, pp. 345-355.

Marques, F.; Lopez, J. M. (1997): Taylor-Couette flow

with axial oscillations of the inner cylinder: Floquet analysis of the basic flow, *J. Fluid Mechanics*, vol. 348, pp. 153-175.

Myong, H. K.; Kasagi, N. (1990): A New Approach to the Improvement of k-ε Turbulence Model for Wall-Bounded Shear Flows, *JSME Int. J.,* Ser. II, vol. 33, no. 1, pp. 63-72.

Patankar, S. V. (1980): Numerical Heat Transfer and Fluid Flow, Hemisphere Pub.

Rodi, W. (1982): Examples of Turbulence Models for Incompressible Flows, *AIAA, J.*, vol. 20, pp. 872-879.

Shigechi, T.; Kawae, N.; Lee, Y. (1990): Turbulent fluid flow and heat transfer in concentric annuli with moving cores, *Int. J. Heat Mass Transfer*, vol. 33, no. 9, 2029-2037.

Tsai, C.C.; Young, D.L.;Cheng, A.H.-D.(2002): Meshless BEM for Three-dimensional Stokes Flows *CMES: Computer Modeling in Engineering & Sciences*, Vol. 3, No. 1, pp. 117-128

Torii, S.; Shimizu, A.; Hasegawa, S.; Kusama, N. (1991): Laminarization of Strongly Heated Annular Gas Flows, *JSME Int. J.*, Ser. II, vol. 34, no. 2, pp. 157-168.

Torii, S.; Yang, W. J. (1994a): A Numerical Study on Turbulent Couette Flow and Heat Transfer in Concentric Annuli, *Int. J. Numerical Methods for Heat & Fluid Flow*, vol. 4, no. 4, pp. 367-377.

Torii, S.; Yang, W. J. (1994b): A Numerical Study on Turbulent Flow and Heat Transfer in Circular Couette Flows, *Numerical Heat Transfer*, Part A, vol. 26, pp. 231-336.

Torii, S.; Yang, W.-J. (1997): Laminarization of Turbulent Gas Flows inside a Strongly Heated Tube, *Int. J. Heat Mass Transfer,* vol. 40, no. 13, pp. 3105-3118.

Wu, J.; Senocak, I.; Wang, G.; Wu, Y.;Shyy, W. (2003): Three-Dimensional Simulation of Turbulent Cavitating Flows in a Hollow-Jet Valve, *CMES: Computer Modeling in Engineering & Sciences*, Vol. 4, No. 6, pp. 679-690.

Youssef, M. S.; Nagano, Y.; Tagawa, M. (1992): A Two-Equation Heat Transfer Model for Predicting Turbulent Thermal Fields under Arbitrary Wall Thermal Conditions, *Int. J. Heat Mass Transfer*, vol. 35, No. 11, pp. 3095-3104.